Fragmentation of electric dipole strength in $N = 82$ isotones

Mitsuru Tohyama[1] and Takashi Nakatsukasa[2,3]

[1] *Kyorin University School of Medicine, Mitaka, Tokyo 181-8611, Japan*
[2] *RIKEN Nishina Center, Wako, Saitama 351-0198, Japan*
[3] *Center for Computational Sciences, University of Tsukuba, Tsukuba 305-8571, Japan*

Fragmentation of the dipole strength in the $N = 82$ isotones ^{140}Ce, ^{142}Nd and ^{144}Sm is calculated using the second random-phase approximation (SRPA). In comparison with the result of the random-phase approximation (RPA), the SRPA provides the additional damping of the giant dipole resonance and the redistribution of the low-energy dipole strength. Properties of the low-energy dipole states are significantly changed by the coupling to two-particle-two-hole ($2p2h$) states, which are also sensitive to the correlation among the $2p2h$ states. Comparison with available experimental data shows a reasonable agreement for the low-energy $E1$ strength distribution.

PACS numbers: 21.60.Jz, 24.30.Cz, 27.60.+j

The low-energy dipole states, often referred to as the pygmy dipole resonance (PDR), have attracted recent experimental [1–6] and theoretical interests [7–12] (see also the recent review [13] and references therein). It is also of significant astrophysical interest, since the low-energy dipole strengths close to the neutron threshold strongly affect the astrophysical r-process nucleosynthesis [14].

The quasiparticle random-phase approximation based on the Hartree-Fock-Bogoliubov ground state (HFB+QRPA) has been extensively used to study the PDR as well as the giant dipole resonances (GDR). Recent systematic calculations [15] for the Nd and Sm isotopes show that although the HFB+QRPA nicely reproduces characteristic features of the shape phase transition in the GDR, it fails to produce the low-energy dipole strengths at $E_x = 5.5 \sim 8$ MeV, observed in the $N = 82$ isotones, ^{142}Nd and ^{144}Sm [1, 3]. The disagreement suggests that the coupling to complex configurations, such as multi-particle-multi-hole states, are required to study the PDR in these nuclei. In fact, the quasiparticle-phonon model (QPM), which takes into account coupling to multi-phonon states, successfully reproduces the low-energy dipole strengths in the $N = 82$ nuclei [2, 4]. A similar approach based on the relativistic mean-field model has also been used to study the PDR in the tin and nickel isotopes [16]. These models assume the multi-phonon characters of the complex states and violate the Pauli principle. Thus, it is desirable to study properties of the PDR with a method complementary to these phonon-coupling approaches. In this work, we present studies for the dipole excitations in the $N = 82$ isotones, with the second random-phase approximation (SRPA) (Ref. [17] and references therein). The SRPA explicitly incorporates the two-particle-two-hole ($2p2h$) states instead of "two-phonon" states, and respects the Pauli principle in the $2p2h$ configurations. Recently, the low-energy dipole states in ^{40,48}Ca have been studied with the SRPA [18], which suggests that the coupling between one-particle-one-hole ($1p1h$) and $2p2h$ configurations enhances the electric dipole ($E1$) strength in the energy range from 5 to 10 MeV. We investigate whether a similar effect can be observed in the isotones of $N = 82$. Since there are many dipole states with small $E1$ strengths in the energy region below 8 MeV, it is difficult to compare property of each state with the experiment. Thus, we perform the comparison of integrated properties at low energies.

The SRPA equation is written in the matrix form[17]

$$\begin{pmatrix} a & c \\ b & d \end{pmatrix} \begin{pmatrix} x^\mu \\ X^\mu \end{pmatrix} = \omega_\mu \begin{pmatrix} x^\mu \\ X^\mu \end{pmatrix}, \qquad (1)$$

where x^μ_{ph} and $X^\mu_{pp'hh'}$ ($p \leftrightarrow h$) are the $1p1h$ and $2p2h$ transition amplitudes for an excited state with an excitation energy ω_μ. The explicit expression for the matrices a, b, c, and d are given in Ref. [19].

The Skyrme interaction of the SIII parameter set is used to calculate the Hartree-Fock single-particle states. The continuum states are discretized by confining the single-particle wave functions in a sphere of radius of 20 fm. Single-particle states with the angular momenta $j_\alpha \leq 15/2$ up to 30 MeV in energy ($\epsilon_\alpha < 30$ MeV) are adopted for the $1p1h$ space (x^μ_{ph} and x^μ_{hp}), both for protons and neutrons. This roughly amounts to one hundred single-particle states. For the $2p2h$ amplitudes ($X^\mu_{pp'hh'}$ and $X^\mu_{hh'pp'}$), we truncate the space into the one made of the single-particle states near the Fermi level, the $2p_{3/2}$, $2p_{1/2}$, $1g_{9/2}$, $1g_{7/2}$, $2d_{5/2}$, $2d_{3/2}$, $3s_{1/2}$, $1h_{11/2}$, and $1h_{9/2}$ orbits for protons and the $2d_{5/2}$, $2d_{3/2}$, $1h_{11/2}$, $1h_{9/2}$, $2f_{7/2}$, and $1i_{13/2}$ orbits for neutrons. The proton orbits up to the $1g_{7/2}$ orbit are assumed to be fully occupied in the ground state of ^{140}Ce, while the proton $2d_{5/2}$ orbit is to be partially occupied in the ground states of ^{142}Nd and ^{144}Sm. The numbers of $1p1h$ and $2p2h$ amplitudes in the SRPA are about 800 and 9000, respectively.

For calculation of the SRPA matrix elements, we employ a residual interaction of the t_0 and t_3 terms of the SIII interaction. Since the residual interaction is not fully consistent with the one used in the calculation of the single-particle states, it is necessary to adjust the strength of the residual interaction so that the spurious mode corresponding to the center-of-mass (COM) motion comes at zero excitation energy in the RPA. This condition determines the renormalization factor f for the resid-

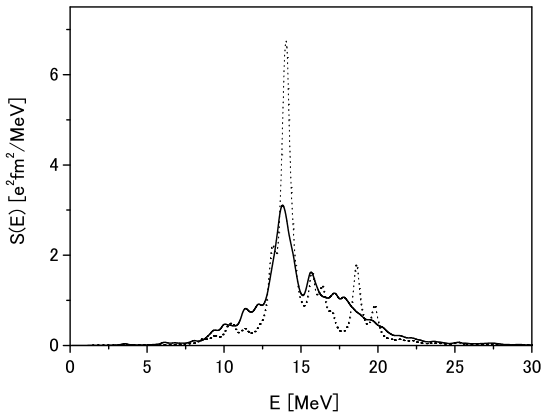

FIG. 1. Strength functions calculated in the SRPA (solid line) and RPA (dotted line) for ^{140}Ce. An artificial width $\Gamma = 0.5$ MeV is used for smoothing. See text for details.

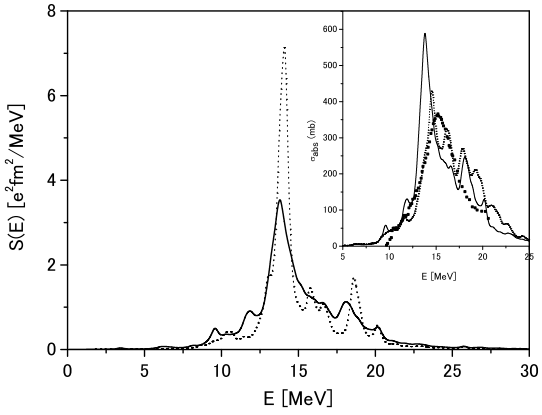

FIG. 2. Same as Fig. 1 but for ^{142}Nd. In the inset the total photoabsorption cross section calculated from the strength function in the SRPA (solid line) is compared with the experimental data (dots) [20]. The dotted line in the inset denotes the result calculated with $f = 0.9$.

ual interaction ($t_0 \to f \times t_0$ and $t_3 \to f \times t_3$). We obtain $f = 0.73$ for ^{142}Nd, and similar values for other nuclei as well. Since the coupling between the spurious COM motion and $2p2h$ configurations is weak, these renormalization factors may approximately produce zero energy in the SRPA as well. Thus, we use this interaction for the calculation of the matrices a, b, and c in Eq. (1). For the residual interaction for the matrix d, following a prescription in Ref. [19], we introduce a zero-range interaction $v_0\delta^3(\boldsymbol{r} - \boldsymbol{r}')$ in addition to the original t_0 and t_3 terms, then, fix the parameter v_0 by approximately reproducing the excitation energy of the lowest 1^- state in ^{142}Nd ($v_0 = -570$ MeV fm^3). With these residual interactions in the given model space, the spurious mode appears at a small imaginary energy ($\omega^2 \approx -1$ MeV^2) in the SRPA.

We first show the results for the GDR. The $E1$ strength functions, $S(E) \equiv \sum_n |\langle n|rY_{1\mu}|0\rangle|^2\delta(E - E_n) = dB(E1; 1^- \to 0^+_{\rm gs})/dE$, calculated in the SRPA (solid line) and RPA (dotted line) for ^{140}Ce, ^{142}Nd, and ^{144}Sm are shown in Figs. 1, 2 and 3, respectively. We use the $E1$ operator with the recoil charges, Ne/A for protons and $-Ze/A$ for neutrons, for the calculation of $S(E)$. The obtained discrete strength functions are smoothed with a small width ($\Gamma = 0.5$ MeV) of Lorentzian. The energy-weighted strength summed up to 50 MeV exhausts 87% of the energy-weighted sum-rule value including the enhancement term arising from the momentum-dependent parts of the Skyrme interaction. The strength distributions of the GDR in the SRPA are broadened, compared to the RPA, due to the coupling to the $2p2h$ states. In the inset of Fig. 2, the total photoabsorption cross section (solid line) calculated in the SRPA is compared with the experimental data [20]. The shape of the GDR depends on the parameter f, whereas it is little affected by the parameter v_0. The GDR peak position and the profile are better described by a slightly larger value of

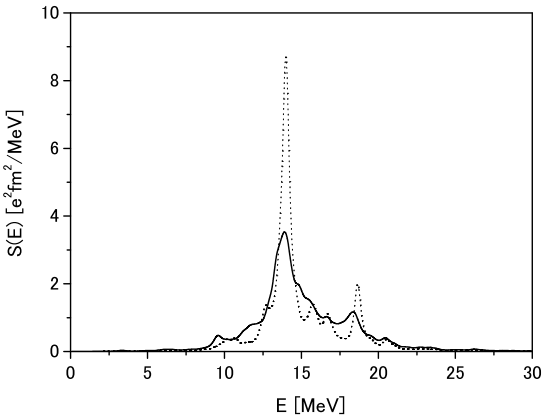

FIG. 3. Same as Fig. 1 but for ^{144}Sm.

f (See the dotted line in the inset of Fig. 2). Our calculation indicates that the coupling to the $2p2h$ induces an additional broadening due to the spreading width, however, the peak position is close to that obtained in the RPA calculation. This is very different from the recent SRPA calculation for ^{16}O in Ref. [21], which indicates a large shift of the GDR peak energy (more than 5 MeV) but almost no broadening. At present, we do not fully understand the origin of this discrepancy. More quantitative analysis of the GDR require an improvement of the present calculation, especially, a self-consistent treatment of the residual interaction and the enlargement of the $2p2h$ space.

Next, let us discuss the low-energy $E1$ strengths. In contrast to the GDR at high energy, the truncation of the $2p2h$ configurations is supposed to be less serious. The $E1$ strengths, $B(E1)\downarrow$, below 10 MeV in ^{140}Ce,

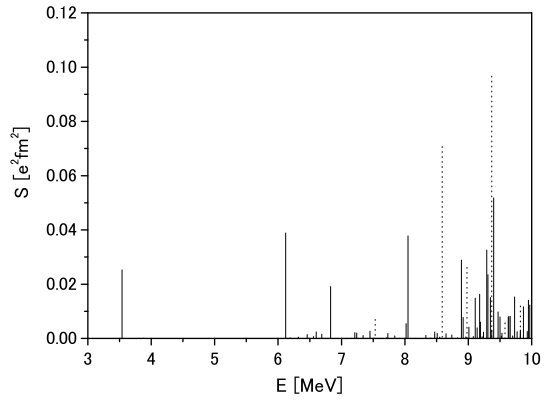

FIG. 4. Low-energy $E1$ strength distributions, $B(E1; 1^- \rightarrow 0^+_{\rm gs})$ calculated in the SRPA (solid line) and RPA (dotted line) for ^{140}Ce.

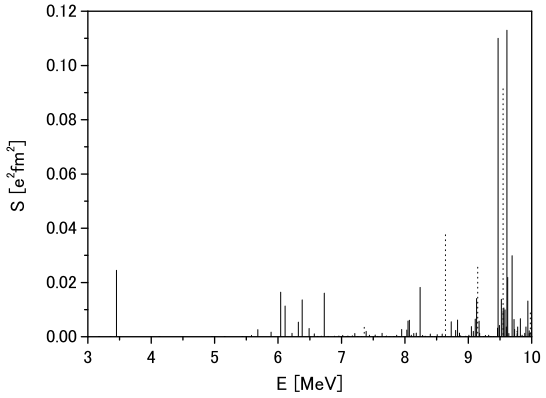

FIG. 5. Same as Fig. 4 but for ^{142}Nd.

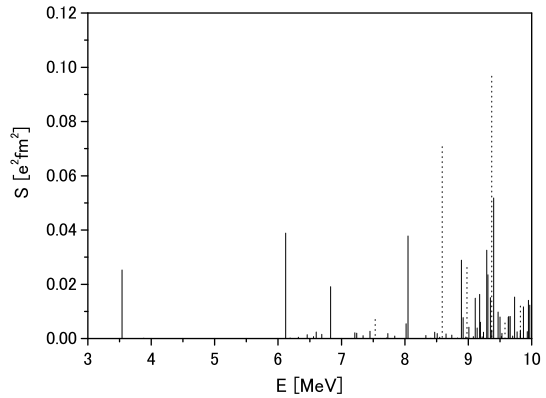

FIG. 6. Same as Fig. 4 but for ^{144}Sm.

TABLE I. Mean energies $\bar{E}$ and summed $B(E1)\uparrow$ values for the low-energy dipole states. The experimental values are taken from Ref. [3]. See text for details.

	$\bar{E}_x$ [MeV]			$\sum B(E1)\uparrow$ [e^2fm^2]		
Nucleus	RPA	SRPA	Exp	RPA	SRPA	Exp
^{140}Ce	7.53	6.47	6.28	0.021	0.219	0.308
^{142}Nd	-	6.31	6.07	0.0	0.224	0.184
^{144}Sm	-	6.04	5.69	0.0	0.233	0.208

^{142}Nd, and ^{144}Sm are shown in Figs. 4, 5, and 6, respectively. In the RPA calculation, there is very little $E1$ strength in the energy region below 8 MeV, which agrees with the result of the QRPA calculation [15]. However, this is different from the experimental findings [1–4]. In the SRPA calculation, the coupling to the $2p2h$ configurations leads to a considerable $E1$ strength in this energy region. To make a quantitative comparison with experiment, the mean excitation energies and the summed $B(E1)\uparrow$ values for low-energy dipole states are calculated in the same way as the experiment [3]: The mean energy is defined as $\bar{E} \equiv \sum EB(E1)/\sum B(E1)$, in which the summation is performed for the dipole states below 7.7 MeV for ^{140}Ce, those below 7.1 MeV for ^{142}Nd, and below 7.0 MeV for ^{144}Sm. The lowest 1^-_1 states are excluded in the summation. The result is tabulated in Table I. For comparison, the RPA values, which include the lowest 1^- state, are listed in the table, but no 1^- state is predicted below 7.1 MeV for ^{142}Nd and ^{144}Sm. Although the calculated mean energies are slightly larger than the observed values, their isotone dependence is consistent with the experiment and the summed transition probabilities are comparable to the experimental values [3].

In the RPA calculation, the neutron excitations are dominant in the low-lying states [13]. The present RPA calculation also indicates, for instance in ^{142}Nd, that the largest components of the low-lying dipole states located at $E_x = 7.36$, 8.64, 9.15, and 9.55 MeV are $(2p_{1/2} \rightarrow 2d_{3/2})\pi$, $(3s_{1/2} \rightarrow 3p_{3/2})\nu$, $(3s_{1/2} \rightarrow 3p_{3/2})\nu$, and $(3s_{1/2} \rightarrow 3p_{1/2})\nu$, respectively. In the SRPA, we see a significant fragmentation of the dipole strength into the energy range of $5 < E < 8$ MeV, in addition to the emergence of the lowest 1^-_1 state at $E \approx 3.5$ MeV. Many of these low-lying dipole states consist of proton $2p2h$ characters, such as $([1g_{7/2}2d_{5/2}]^{6^+} \rightarrow [1h_{11/2}2d_{3/2}]^{7^-})\pi$ and $([1g_{7/2}2d_{5/2}]^{6^+} \rightarrow [1h_{11/2}3s_{1/2}]^{5^-})\pi$. These proton $2p2h$ configurations come down to the lower energy because of the coupling to the $2p2h$ configurations consisting of the neutron $1p1h$ transition from the $1h_{11/2}$ orbit to the $1h_{9/2}$ orbit and the proton $1p1h$ transitions from the $1g_{7/2}$ orbit (or $2d_{5/2}$ orbit) to the $1h_{11/2}$ orbit; $\pi 1g_{7/2}\nu 1h_{11/2} \rightarrow \pi 1h_{11/2}\nu 1h_{9/2}$ and. $\pi 2d_{5/2}\nu 1h_{11/2} \rightarrow \pi 1h_{11/2}\nu 1h_{9/2}$ and. We have confirmed the importance of these proton-neutron $2p2h$ configurations by performing the SRPA calculation in a smaller $2p2h$ space. The SRPA calculation with the neutron $1h$ orbits qualita-

TABLE II. Excitation energies E and $B(E1;0^+_{\rm gs} \to 1^-)$ of the lowest 1^- states. Note that the energy of the 1^-_1 state in ^{142}Nd was approximately fitted by adjusting the parameter v_0. The experimental values are taken from Ref. [3].

	E [MeV]			$B(E1)\uparrow$ [e^2fm^2]		
Nucleus	RPA	SRPA	Exp	RPA	SRPA	Exp
^{140}Ce	7.53	3.54	3.644	0.021	0.076	0.0217
^{142}Nd	7.36	3.45	3.424	0.010	0.074	0.0211
^{144}Sm	7.18	3.35	3.226	0.004	0.068	0.0248

tively produces the same result.

Finally, let us discuss the property of the lowest 1^- state. The excitation energies and the reduced transition probabilities $B(E1)\uparrow$ of the 1^-_1 states in ^{140}Ce, ^{142}Nd and ^{144}Sm are compared with the experimental values [3] in Table II. The calculated excitation energies decrease with increasing proton number, which is consistent with the experiment. However, the SRPA calculations overestimate the $B(E1)\uparrow$ values by a factor of $2.7-3.5$. The structure of the 1^-_1 states in these nuclei is supposed to be predominantly of the two-phonon quadrupole-octupole character $2^+\otimes 3^-$ [1, 3]. However, in the present SRPA calculation, the $2p2h$ configuration ($[\pi 1g_{7/2}\nu 1h_{11/2}]^{1^-} \to [\pi 1h_{11/2}\nu 1h_{9/2}]^{2^+}$) is dominant in these 1^-_1 states, which differs from the two-phonon $2^+\otimes 3^-$ character. The pairing correlation, which is not taken into account in the present calculation, may play an important role for a better description of the two-phonon character of the 1^-_1 states, because they are essential in the description of the lowest quadrupole and octupole states. Furthermore, it has been known that the SRPA fails to describe the collectivity of the two-phonon states [22]. This is due to the fact that the next-leading terms in the two-phonon state are missing in the SRPA. These missing terms beyond the SRPA can be taken into account by introducing $X_{php'h'}$ amplitudes in Eq. (1). A general equation for the extended RPA formalism with the ground-state correlation is given in Ref. [23]. Another possible method to improve the description of the two-phonon states is the dressed-four-quasi-particle approach proposed in Ref. [24]. These are beyond the scope of the present work, but of significant interest in future.

In summary, the fragmentation of the dipole strength in the $N = 82$ isotones, ^{142}Nd, ^{142}Nd and ^{144}Sm, was studied using the second random-phase approximation (SRPA). The SRPA successfully produces the spreading of the giant dipole resonance and the concentration of the dipole strength in the low-energy region, simultaneously. However, the transition strength of the first dipole state was overestimated in the SRPA, indicating the necessity of a more elaborate treatment for the states with the two-phonon character. The calculation based on the extended RPA with the ground-state correlations is of great interest and currently under progress.

This work is supported by Grant-in-Aid for Scientific Research on Innovative Areas (No. 20105003) and by the Grant-in-Aid for Scientific Research(B) (No. 21340073).

[1] A. Zilges *et al.*, Phys. Lett. B **542**, 43 (2002).
[2] J. Enders, et al., Nucl. Phys. A **741**, 3 (2004).
[3] S. Volz *et al.*, Nucl. Phys. A **779**, 1 (2006).
[4] D. Savran *et al.*, Phys. Rev. Lett. **100**, 232501 (2008).
[5] R. Schwengner *et al.*, Phys. Rev. C **76**, 034321 (2007).
[6] O. Wieland *et al.*, Phys. Rev. Lett. **102**, 092502 (2009).
[7] K. Yoshida and N. Van Giai, Phys. Rev. C **78**, 064316 (2008).
[8] D. Peña Arteaga and P. Ring, Phys. Rev. **C 77**, 034317 (2008); D. Peña Arteaga et al., Phys. Rev. **C 79**, 034311 (2009).
[9] N. Paar, et al., Phys. Rev. Lett. **103**, 032502 (2009).
[10] S. Ebata et al.. Phys. Rev. C **82**, 034306 (2010).
[11] T. Inakura, T. Nakatsukasa, and K. Yabana, Phys. Rev. C **84**, 021302 (2011).
[12] M. Martini et al., Phys. Rev. **C 83**, 034309 (2011).
[13] N. Paar, D. Vretenar, E. Khan, and G. Coló, Rep. Prog. Phys. **70**, 691 (2007).
[14] S. Goriely and E. Khan, Nucl. Phys. A**706**, 217 (2002).
[15] K. Yoshida and T. Nakatsukasa, Phys. Rev. C**83**, 021304 (R) (2011).
[16] E. Litvinova, P. Ring and V. Tselyaev, Phys. Rev. Lett. **105**, 022502 (2010).
[17] S. Drożdż, S. Nishizaki, J. Speth and J. Wambach, Phys. Rep. **197**, 1 (1990).
[18] D. Gambacurta, M. Grasso, and F. Catara, Phys. Rev. C **84**, 034301 (2011).
[19] M. Tohyama, Phys. Rev. C **75**, 044310 (2007).
[20] P. Carlos, H. Beil, R. Bergere, A. Lepretre and A. Veyssiere, Nucl. Phys. A**172**, 437 (1971).
[21] D. Gambacurta, M. Grasso, and F. Catara, Phys. Rev. C **81**, 054312 (2010).
[22] T. Tamura and T. Udagawa, Nucl. Phys. **53**, 33 (1964).
[23] M. Tohyama and P. Schuck, Eur. Phys. J. A**32**, 139 (2007).
[24] N. Kanesaki, T. Marumori, F. Sakata, and K. Takada, Prog. Theor. Phys. **49**, 181 (1973); **50**, 867 (1973).